

Evidence for Direct CP Violation in $B^0 \rightarrow K^+ \pi^-$ Decays

Y. Chao,²⁹ P. Chang,²⁹ K. Abe,¹⁰ K. Abe,⁴⁶ N. Abe,⁴⁹ I. Adachi,¹⁰ H. Aihara,⁴⁸ K. Akai,¹⁰ M. Akatsu,²⁴ M. Akemoto,¹⁰ Y. Asano,⁵³ T. Aso,⁵² V. Aulchenko,² T. Aushev,¹⁴ T. Aziz,⁴⁴ S. Bahinipati,⁶ A. M. Bakich,⁴³ Y. Ban,³⁶ M. Barbero,⁹ A. Bay,²⁰ I. Bedny,² U. Bitenc,¹⁵ I. Bizjak,¹⁵ S. Blyth,²⁹ A. Bondar,² A. Bozek,³⁰ M. Bračko,^{22,15} J. Brodzicka,³⁰ T. E. Browder,⁹ M.-C. Chang,²⁹ A. Chen,²⁶ K.-F. Chen,²⁹ W. T. Chen,²⁶ B. G. Cheon,⁴ R. Chistov,¹⁴ S.-K. Choi,⁸ Y. Choi,⁴² Y. K. Choi,⁴² A. Chuvikov,³⁷ S. Cole,⁴³ M. Danilov,¹⁴ M. Dash,⁵⁵ L. Y. Dong,¹² R. Dowd,²³ J. Dragic,²³ A. Drutskoy,⁶ S. Eidelman,² V. Eiges,¹⁴ Y. Enari,²⁴ D. Epifanov,² C. W. Everton,²³ F. Fang,⁹ J. Flanagan,¹⁰ S. Fratina,¹⁵ H. Fujii,¹⁰ Y. Funakoshi,¹⁰ K. Furukawa,¹⁰ N. Gabyshev,² A. Garmash,³⁷ T. Gershon,¹⁰ A. Go,²⁶ G. Gokhroo,⁴⁴ B. Golob,^{21,15} M. Grosse Perdekamp,³⁸ H. Guler,⁹ R. Guo,²⁷ J. Haba,¹⁰ C. Hagner,⁵⁵ F. Handa,⁴⁷ K. Hara,³⁴ T. Hara,³⁴ N. C. Hastings,¹⁰ K. Hasuko,³⁸ K. Hayasaka,²⁴ H. Hayashii,²⁵ M. Hazumi,¹⁰ E. M. Heenan,²³ I. Higuchi,⁴⁷ T. Higuchi,¹⁰ L. Hinz,²⁰ T. Hojo,³⁴ T. Hokuue,²⁴ Y. Hoshi,⁴⁶ K. Hoshina,⁵¹ S. Hou,²⁶ W.-S. Hou,²⁹ Y. B. Hsiung,²⁹ H.-C. Huang,²⁹ T. Igaki,²⁴ Y. Igarashi,¹⁰ T. Iijima,²⁴ H. Ikeda,¹⁰ A. Imoto,²⁵ K. Inami,²⁴ A. Ishikawa,¹⁰ H. Ishino,⁴⁹ K. Itoh,⁴⁸ R. Itoh,¹⁰ M. Iwamoto,³ M. Iwasaki,⁴⁸ Y. Iwasaki,¹⁰ R. Kagan,¹⁴ H. Kakuno,⁴⁸ T. Kamitani,¹⁰ J. H. Kang,⁵⁶ J. S. Kang,¹⁷ P. Kapusta,³⁰ S. U. Kataoka,²⁵ N. Katayama,¹⁰ H. Kawai,³ H. Kawai,⁴⁸ Y. Kawakami,²⁴ N. Kawamura,¹ T. Kawasaki,³² N. Kent,⁹ H. R. Khan,⁴⁹ A. Kibayashi,⁴⁹ H. Kichimi,¹⁰ M. Kikuchi,¹⁰ E. Kikutani,¹⁰ H. J. Kim,¹⁹ H. O. Kim,⁴² Hyunwoo Kim,¹⁷ J. H. Kim,⁴² S. K. Kim,⁴¹ T. H. Kim,⁵⁶ K. Kinoshita,⁶ S. Kobayashi,³⁹ H. Koiso,¹⁰ P. Koppenburg,¹⁰ S. Korpar,^{22,15} P. Križan,^{21,15} P. Krokovny,² T. Kubo,¹⁰ R. Kulasiri,⁶ S. Kumar,³⁵ C. C. Kuo,²⁶ H. Kurashiro,⁴⁹ E. Kurihara,³ A. Kusaka,⁴⁸ A. Kuzmin,² Y.-J. Kwon,⁵⁶ J. S. Lange,⁷ G. Leder,¹³ S. E. Lee,⁴¹ S. H. Lee,⁴¹ Y.-J. Lee,²⁹ T. Lesiak,³⁰ J. Li,⁴⁰ A. Limosani,²³ S.-W. Lin,²⁹ D. Liventsev,¹⁴ J. MacNaughton,¹³ G. Majumder,¹³ F. Mandl,¹³ D. Marlow,³⁷ M. Masuzawa,¹⁰ T. Matsuiishi,²⁴ H. Matsumoto,³² S. Matsumoto,⁵ T. Matsumoto,⁵⁰ A. Matyja,³⁰ S. Michizono,¹⁰ Y. Mikami,⁴⁷ T. Mimashi,¹⁰ W. Mitaroff,¹³ K. Miyabayashi,²⁵ Y. Miyabayashi,²⁴ H. Miyake,³⁴ H. Miyata,³² R. Mizuk,¹⁴ D. Mohapatra,⁵⁵ G. R. Moloney,²³ G. F. Moorhead,²³ T. Mori,⁴⁹ J. Mueller,¹⁰ A. Murakami,³⁹ T. Nagamine,⁴⁷ Y. Nagasaka,¹¹ T. Nakadaira,⁴⁸ I. Nakamura,¹⁰ T. T. Nakamura,¹⁰ E. Nakano,³³ M. Nakao,¹⁰ H. Nakayama,¹⁰ H. Nakazawa,¹⁰ Z. Natkaniec,³⁰ K. Neichi,⁴⁶ S. Nishida,¹⁰ O. Nitoh,⁵¹ S. Noguchi,²⁵ T. Nozaki,¹⁰ A. Ogawa,³⁸ S. Ogawa,⁴⁵ Y. Ogawa,¹⁰ K. Ohmi,¹⁰ Y. Ohnishi,¹⁰ T. Ohshima,²⁴ N. Ohuchi,¹⁰ K. Oide,¹⁰ T. Okabe,²⁴ S. Okuno,¹⁶ S. L. Olsen,⁹ Y. Onuki,³² W. Ostrowicz,³⁰ H. Ozaki,¹⁰ P. Pakhlov,¹⁴ H. Palka,³⁰ C. W. Park,⁴² H. Park,¹⁹ K. S. Park,⁴² N. Parslow,⁴³ L. S. Peak,⁴³ M. Pernicka,¹³ J.-P. Perroud,²⁰ M. Peters,⁹ L. E. Piilonen,⁵⁵ A. Poluektov,² F. J. Ronga,¹⁰ N. Root,² M. Rozanska,³⁰ H. Sagawa,¹⁰ M. Saigo,⁴⁷ S. Saitoh,¹⁰ Y. Sakai,¹⁰ H. Sakamoto,¹⁸ H. Sakaue,³³ T. R. Sarangi,¹⁰ M. Satapathy,⁵⁴ N. Sato,²⁴ T. Schietinger,²⁰ O. Schneider,²⁰ J. Schümann,²⁹ C. Schwanda,¹³ A. J. Schwartz,⁶ T. Seki,⁵⁰ S. Semenov,¹⁴ K. Senyo,²⁴ Y. Settai,⁵ R. Seuster,⁹ M. E. Sevior,²³ T. Shibata,³² H. Shibuya,⁴⁵ T. Shidara,¹⁰ B. Shwartz,² V. Sidorov,² V. Siegle,³⁸ J. B. Singh,³⁵ A. Somov,⁶ N. Soni,³⁵ R. Stamen,¹⁰ S. Stanič,^{53,*} M. Starič,¹⁵ R. Sugahara,¹⁰ A. Sugi,²⁴ T. Sugimura,¹⁰ A. Sugiyama,³⁹ K. Sumisawa,³⁴ T. Sumiyoshi,⁵⁰ S. Suzuki,³⁹ S. Y. Suzuki,¹⁰ S. K. Swain,⁹ O. Tajima,¹⁰ F. Takasaki,¹⁰ K. Tamai,¹⁰ N. Tamura,³² K. Tanabe,⁴⁸ M. Tanaka,¹⁰ M. Tawada,¹⁰ G. N. Taylor,²³ Y. Teramoto,³³ X. C. Tian,³⁶ S. Tokuda,²⁴ S. N. Tovey,²³ K. Trabelsi,⁹ T. Tsuboyama,¹⁰ T. Tsukamoto,¹⁰ K. Uchida,⁹ S. Uehara,¹⁰ T. Uglov,¹⁴ K. Ueno,²⁹ Y. Unno,³ S. Uno,¹⁰ Y. Ushiroda,¹⁰ G. Varner,⁹ K. E. Varvell,⁴³ S. Villa,²⁰ C. C. Wang,²⁹ C. H. Wang,²⁸ J. G. Wang,⁵⁵ M.-Z. Wang,²⁹ M. Watanabe,³² Y. Watanabe,⁴⁹ L. Widhalm,¹³ Q. L. Xie,¹² B. D. Yabsley,⁵⁵ A. Yamaguchi,⁴⁷ H. Yamamoto,⁴⁷ N. Yamamoto,¹⁰ S. Yamamoto,⁵⁰ T. Yamanaka,³⁴ Y. Yamashita,³¹ M. Yamauchi,¹⁰ Heyoung Yang,⁴¹ P. Yeh,²⁹ J. Ying,³⁶ K. Yoshida,²⁴ M. Yoshida,¹⁰ Y. Yuan,¹² Y. Yusa,⁴⁷ H. Yuta,¹ S. L. Zang,¹² C. C. Zhang,¹² J. Zhang,¹⁰ L. M. Zhang,⁴⁰ Z. P. Zhang,⁴⁰ Y. Zheng,⁹ V. Zhilich,² T. Ziegler,³⁷ D. Žontar,^{21,15} and D. Zürcher²⁰

(Belle Collaboration)

¹Aomori University, Aomori²Budker Institute of Nuclear Physics, Novosibirsk³Chiba University, Chiba⁴Chonnam National University, Kwangju⁵Chuo University, Tokyo⁶University of Cincinnati, Cincinnati, Ohio 45221⁷University of Frankfurt, Frankfurt⁸Gyeongsang National University, Chinju

- ⁹University of Hawaii, Honolulu, Hawaii 96822
¹⁰High Energy Accelerator Research Organization (KEK), Tsukuba
¹¹Hiroshima Institute of Technology, Hiroshima
¹²Institute of High Energy Physics, Chinese Academy of Sciences, Beijing
¹³Institute of High Energy Physics, Vienna
¹⁴Institute for Theoretical and Experimental Physics, Moscow
¹⁵J. Stefan Institute, Ljubljana
¹⁶Kanagawa University, Yokohama
¹⁷Korea University, Seoul
¹⁸Kyoto University, Kyoto
¹⁹Kyungpook National University, Taegu
²⁰Swiss Federal Institute of Technology of Lausanne, EPFL, Lausanne
²¹University of Ljubljana, Ljubljana
²²University of Maribor, Maribor
²³University of Melbourne, Victoria
²⁴Nagoya University, Nagoya
²⁵Nara Women's University, Nara
²⁶National Central University, Chung-li
²⁷National Kaohsiung Normal University, Kaohsiung
²⁸National United University, Miao Li
²⁹Department of Physics, National Taiwan University, Taipei
³⁰H. Niewodniczanski Institute of Nuclear Physics, Krakow
³¹Nihon Dental College, Niigata
³²Niigata University, Niigata
³³Osaka City University, Osaka
³⁴Osaka University, Osaka
³⁵Panjab University, Chandigarh
³⁶Peking University, Beijing
³⁷Princeton University, Princeton, New Jersey 08545
³⁸RIKEN BNL Research Center, Upton, New York 11973
³⁹Saga University, Saga
⁴⁰University of Science and Technology of China, Hefei
⁴¹Seoul National University, Seoul
⁴²Sungkyunkwan University, Suwon
⁴³University of Sydney, Sydney NSW
⁴⁴Tata Institute of Fundamental Research, Bombay
⁴⁵Toho University, Funabashi
⁴⁶Tohoku Gakuin University, Tagajo
⁴⁷Tohoku University, Sendai
⁴⁸Department of Physics, University of Tokyo, Tokyo
⁴⁹Tokyo Institute of Technology, Tokyo
⁵⁰Tokyo Metropolitan University, Tokyo
⁵¹Tokyo University of Agriculture and Technology, Tokyo
⁵²Toyama National College of Maritime Technology, Toyama
⁵³University of Tsukuba, Tsukuba
⁵⁴Utkal University, Bhubaneswer
⁵⁵Virginia Polytechnic Institute and State University, Blacksburg, Virginia 24061
⁵⁶Yonsei University, Seoul

(Received 20 August 2004; published 5 November 2004)

We report evidence for direct CP violation in the decay $B^0 \rightarrow K^+ \pi^-$ with 253 fb^{-1} of data collected with the Belle detector at the KEKB $e^+ e^-$ collider. Using $275 \times 10^6 B\bar{B}$ pairs we observe a $B \rightarrow K^\pm \pi^\mp$ signal with 2140 ± 53 events. The measured CP violating asymmetry is $\mathcal{A}_{CP}(K^+ \pi^-) = -0.101 \pm 0.025(\text{stat}) \pm 0.005(\text{syst})$, corresponding to a significance of 3.9σ including systematics. We also search for CP violation in the decays $B^+ \rightarrow K^+ \pi^0$ and $B^+ \rightarrow \pi^+ \pi^0$. The measured CP violating asymmetries are $\mathcal{A}_{CP}(K^+ \pi^0) = 0.04 \pm 0.05(\text{stat}) \pm 0.02(\text{syst})$ and $\mathcal{A}_{CP}(\pi^+ \pi^0) = -0.02 \pm 0.10(\text{stat}) \pm 0.01(\text{syst})$, corresponding to the intervals $-0.05 < \mathcal{A}_{CP}(K^+ \pi^0) < 0.13$ and $-0.18 < \mathcal{A}_{CP}(\pi^+ \pi^0) < 0.14$ at 90% confidence level.

DOI: 10.1103/PhysRevLett.93.191802

PACS numbers: 13.25.Hw, 11.30.Er, 12.15.Hh, 14.40.Nd

In the standard model (SM), CP violation arises via the interference of at least two diagrams with comparable amplitudes but different CP conserving and violating phases. Mixing induced CP violation in the B sector has been established in $b \rightarrow c\bar{c}s$ transitions [1,2]. In the standard model, direct CP violation is also expected to be sizable in the B meson system [3]. The first experimental evidence for direct CP violation in B mesons was shown by Belle for the decay mode $B^0 \rightarrow \pi^+ \pi^-$ [4]. This result suggests large interference between tree and penguin diagrams and the existence of final state interactions [5]. Recently, both Belle [6] and BABAR [7] have reported searches for direct CP violation in another decay mode $B^0 \rightarrow K^+ \pi^-$, where direct CP violation is also expected.

The CP violating partial rate asymmetry is measured as:

$$\mathcal{A}_{CP} = \frac{N(\bar{B} \rightarrow \bar{f}) - N(B \rightarrow f)}{N(\bar{B} \rightarrow \bar{f}) + N(B \rightarrow f)}, \quad (1)$$

where $N(\bar{B} \rightarrow \bar{f})$ is the yield for the $\bar{B} \rightarrow K\pi/\pi\pi$ decay and $N(B \rightarrow f)$ denotes that of the charge-conjugate mode. Theoretical predictions with different approaches suggest that $\mathcal{A}_{CP}(K^+ \pi^-)$ could be either positive or negative [8]. Although there are large uncertainties related to hadronic effects in the theoretical predictions, results for $\mathcal{A}_{CP}(K^+ \pi^-)$ and $\mathcal{A}_{CP}(K^+ \pi^0)$ are expected to have the same sign and be comparable in magnitude [8]. In this Letter, we report \mathcal{A}_{CP} measurements for $B^0 \rightarrow K^+ \pi^-$, $B^+ \rightarrow K^+ \pi^0$ and $B^+ \rightarrow \pi^+ \pi^0$ using 275×10^6 $B\bar{B}$ pairs collected with the Belle detector at the KEKB e^+e^- asymmetric-energy (3.5 on 8 GeV) collider [9] operating at the $\Upsilon(4S)$ resonance.

The Belle detector is a large-solid-angle magnetic spectrometer that consists of a silicon vertex detector (SVD), a 50-layer central drift chamber (CDC), an array of aerogel threshold Cherenkov counters (ACC), a barrel-like arrangement of time-of-flight scintillation counters (TOF), and an electromagnetic calorimeter (ECL) comprised of CsI(Tl) crystals located inside a superconducting solenoid coil that provides a 1.5 T magnetic field. An iron flux-return located outside of the coil is instrumented to detect K_L^0 mesons and to identify muons (KLM). The detector is described in detail elsewhere [10]. Two different inner detector configurations were used. For the first sample of 152×10^6 $B\bar{B}$ pairs (set I), a 2.0 cm radius beampipe and a 3-layer silicon vertex detector were used; for the latter 123×10^6 $B\bar{B}$ pairs (set II), a 1.5 cm radius beampipe, a 4-layer silicon detector, and a small-cell inner drift chamber were used [11].

The B candidate selection is the same as described in Ref. [12]. Charged tracks are required to originate from the interaction point (IP). Charged kaons and pions are identified using dE/dx information and Cherenkov light yields in the ACC. The dE/dx and ACC information are combined to form a K - π likelihood ratio, $\mathcal{R}(K\pi) =$

$\mathcal{L}_K/(\mathcal{L}_K + \mathcal{L}_\pi)$, where \mathcal{L}_K (\mathcal{L}_π) is the likelihood of kaon (pion). Charged tracks with $\mathcal{R}(K\pi) > 0.6$ are regarded as kaons and tracks with $\mathcal{R}(K\pi) < 0.4$ as pions. Furthermore, charged tracks that are positively identified as electrons are rejected. The electron identification uses the information composed of E/p and dE/dx , shower shape, track matching χ^2 , and ACC light yields. The K/π identification efficiencies and misidentification rates are determined from a sample of kinematically identified $D^{*+} \rightarrow D^0 \pi^+$, $D^0 \rightarrow K^- \pi^+$ decays, where the kaon and pion from the D decay are selected in the same kinematic region as in the $B^0 \rightarrow K^+ \pi^-$ decay. Table I shows the results. The detection efficiency for $K^- \pi^+$ is found to be 1.0% greater than that for $K^+ \pi^-$; this small difference is corrected for in the \mathcal{A}_{CP} measurement.

Candidate π^0 mesons are reconstructed by combining two photons with invariant mass between 115 MeV/ c^2 and 152 MeV/ c^2 , which corresponds to ± 2.5 standard deviations around the nominal π^0 mass. Each photon is required to have a minimum energy of 50 MeV in the barrel region ($32^\circ < \theta_\gamma < 129^\circ$) or 100 MeV in the end-cap region ($17^\circ < \theta_\gamma < 32^\circ$ or $129^\circ < \theta_\gamma < 150^\circ$), where θ_γ denotes the polar angle of the photon with respect to the beam line. To further reduce the combinatorial background, π^0 candidates with small decay angles ($\cos\theta^* > 0.95$) are rejected, where θ^* is the angle between the π^0 boost direction in the laboratory frame and its γ daughters in the π^0 rest frame.

Two variables are used to identify B candidates: the beam-constrained mass, $M_{bc} = \sqrt{E_{\text{beam}}^{*2} - p_B^{*2}}$, and the energy difference, $\Delta E = E_B^* - E_{\text{beam}}^*$, where E_{beam}^* is the beam energy and E_B^* and p_B^* are the reconstructed energy and momentum of the B candidates in the center-of-mass (CM) frame. Events with $M_{bc} > 5.20$ GeV/ c^2 and -0.3 GeV $< \Delta E < 0.5$ GeV are selected for the final analysis.

The dominant background is from $e^+e^- \rightarrow q\bar{q}$ ($q = u, d, s, c$) continuum events. To distinguish the signal from the jetlike continuum background, event topology variables and B flavor tagging information are employed. We combine a set of modified Fox-Wolfram moments [13] into a Fisher discriminant. The probability density function (PDF) for this discriminant, and that for the cosine of the angle between the B flight direction and the z axis,

TABLE I. Performance of $K - \pi$ identification measured using $D^{*+} \rightarrow D^0 \pi^+$, $D^0 \rightarrow K^- \pi^+$ decays.

	Set I		Set II	
	Eff. (%)	Fake rate (%)	Eff. (%)	Fake rate (%)
K^+	83.74 ± 0.18	5.10 ± 0.12	82.41 ± 0.20	6.57 ± 0.15
K^-	84.73 ± 0.18	5.69 ± 0.12	83.26 ± 0.20	7.14 ± 0.15
π^+	91.25 ± 0.15	10.74 ± 0.15	89.48 ± 0.18	11.82 ± 0.17
π^-	90.54 ± 0.16	10.09 ± 0.15	88.56 ± 0.19	11.57 ± 0.17

are obtained using signal and continuum Monte Carlo (MC) events. These two variables are then combined to form a likelihood ratio $\mathcal{R} = \mathcal{L}_s / (\mathcal{L}_s + \mathcal{L}_{q\bar{q}})$, where $\mathcal{L}_{s(q\bar{q})}$ is the product of signal ($q\bar{q}$) probability densities. Additional background discrimination is provided by B flavor tagging. The standard Belle flavor tagging algorithm [14] gives two outputs: a discrete variable indicating the flavor of the tagging B and a MC-determined dilution factor r , which ranges from zero for no flavor information to unity for unambiguous flavor assignment. An event with a high value of r (typically containing a high-momentum lepton) is more likely to be a $B\bar{B}$ event so a looser \mathcal{R} requirement can be applied. We divide the data into $r > 0.5$ and $r < 0.5$ regions. The continuum background is reduced by applying a selection requirement on \mathcal{R} for events in each r region of set I and set II according to the figure of merit defined as $N_s^{\text{exp}} / \sqrt{N_s^{\text{exp}} + N_{q\bar{q}}^{\text{exp}}}$, where N_s^{exp} denotes the expected signal yields based on MC simulation and our previous branching fraction measurements [12], and $N_{q\bar{q}}^{\text{exp}}$ denotes the expected $q\bar{q}$ yields from sideband data ($M_{bc} < 5.26 \text{ GeV}/c^2$). A typical requirement suppresses 92%–99% of the continuum background while retaining 48%–67% of the signal.

Backgrounds from $Y(4S) \rightarrow B\bar{B}$ events are investigated using a large MC sample. After the \mathcal{R} requirement, we find a small charmless three-body background at low ΔE and reflections from $B^0 \rightarrow \pi^+\pi^-$ decays due to $K-\pi$ misidentification.

The signal yields are extracted by applying unbinned two-dimensional maximum likelihood (ML) fits to the (M_{bc} and ΔE) distributions of the B and \bar{B} samples. The likelihood for each mode is defined as

$$\mathcal{L} = \exp\left(-\sum_{s,k,j} N_{s,k,j}\right) \times \prod_i \left(\sum_{s,k,j} N_{s,k,j} \mathcal{P}_{s,k,j,i}\right) \quad (2)$$

$$\mathcal{P}_{s,k,j,i} = \frac{1}{2} [1 - q_i \mathcal{A}_{CPj}] P_{s,k,j}(M_{bc,i}, \Delta E_i), \quad (3)$$

where s indicates set I or set II, k distinguishes events in the $r < 0.5$ or $r > 0.5$ regions, i is the identifier of the i -th event, $P(M_{bc}, \Delta E)$ is the two-dimensional PDF of M_{bc} and ΔE , q indicates the B meson flavor, $B(q = +1)$ or $\bar{B}(q = -1)$, N_j is the number of events for the category j , which corresponds to either signal, $q\bar{q}$ continuum, a reflection due to $K-\pi$ misidentification, or background from other charmless three-body B decays.

The yields and asymmetries for the signal and backgrounds are allowed to float in all modes. Since the $K^+\pi^0$ and $\pi^+\pi^0$ reflections are difficult to distinguish with ΔE and M_{bc} , we fit these two modes simultaneously with a fixed reflection-to-signal ratio based on the measured $K-\pi$ identification efficiencies and fake rates. All the signal PDFs ($P(M_{bc}, \Delta E)$) are obtained using MC simulations based on the set I and set II detector configura-

tions. The same signal PDFs are used for events in the two different r regions. No strong correlations between M_{bc} and ΔE are found for the $B \rightarrow K^+\pi^-$ signal. Therefore, its PDF is modeled by a product of a single Gaussian for M_{bc} and a double Gaussian for ΔE . For the modes with neutral pions in the final state, there are correlations between M_{bc} and ΔE in the tails of the signals; hence, their PDFs are described by smoothed two-dimensional histograms. Discrepancies between the signal peak positions in data and MC are calibrated using $B^+ \rightarrow \bar{D}^0 \pi^+$ decays, where the $\bar{D}^0 \rightarrow K^+\pi^-\pi^0$ subdecay is used for the modes with a π^0 meson while $\bar{D}^0 \rightarrow K^+\pi^-$ is used for the $K^+\pi^-$ mode. The MC-predicted ΔE resolutions are verified using the invariant mass distributions of high-momentum D mesons. The decay mode $\bar{D}^0 \rightarrow K^+\pi^-$ is used for $B^0 \rightarrow K^+\pi^-$, and $\bar{D}^0 \rightarrow K^+\pi^-\pi^0$ for the modes with a π^0 in the final state. The parameters that describe the shapes of the PDFs are fixed in all of the fits.

The continuum background in ΔE is described by a first or second order polynomial while the M_{bc} distribution is parameterized by an ARGUS function $f(x) = x\sqrt{1-x^2}\exp[-\xi(1-x^2)]$, where x is M_{bc} divided by half of the total center-of mass energy [15]. The continuum PDF is the product of an Argus function and a polynomial, where ξ and the coefficients of the polynomial are free parameters. These free parameters are r -dependent. A large MC sample is used to investigate the background from charmless B decays and a smoothed two-dimensional histogram is taken as the PDF. The functional forms of the PDFs are the same for the B and \bar{B} samples.

The efficiency of particle identification is slightly different for positively and negatively charged particles; consequently, the raw number of asymmetry in Eq. (3) no longer gives \mathcal{A}_{CP} correctly and must be corrected. For the $K^+\pi^0$ and $\pi^+\pi^0$ modes, this raw asymmetry can be expressed as:

$$\mathcal{A}_{CP}^{\text{raw}} = \frac{\mathcal{A}_\epsilon + \mathcal{A}_{CP}}{1 + \mathcal{A}_\epsilon \mathcal{A}_{CP}}, \quad (4)$$

where \mathcal{A}_{CP} is the true partial rate asymmetry and the efficiency asymmetry \mathcal{A}_ϵ is the efficiency difference between $K^-(\pi^+)$ and $K^+(\pi^-)$ divided by the sum of their efficiencies. The situation is more complicated for the $K^+\pi^-$ mode because, in addition to the bias due to the efficiency difference between $K^-\pi^+$ and $K^+\pi^-$, a $K^-\pi^+$ signal event can be misidentified as a $K^+\pi^-$ candidate and dilute \mathcal{A}_{CP} . The efficiency asymmetry results in an \mathcal{A}_{CP} bias of +0.01 while the small dilution factor due to double misidentification reduces \mathcal{A}_{CP} by a factor of 0.99. These effects are included in the raw asymmetry correction and their errors are included in the systematic uncertainty.

Table II gives the signal yields and \mathcal{A}_{CP} values for each mode. The asymmetries for the background components

TABLE II. Fitted signal yields, \mathcal{A}_{CP} results, and background asymmetries for individual modes.

Mode	Signal Yield	\mathcal{A}_{CP}	Bkg \mathcal{A}_{CP}
$K^\pm \pi^\pm$	2140 ± 53	$-0.101 \pm 0.025 \pm 0.005$	-0.001 ± 0.005
$K^\pm \pi^0$	728 ± 34	$0.04 \pm 0.05 \pm 0.02$	-0.02 ± 0.01
$\pi^\pm \pi^0$	315 ± 29	$-0.02 \pm 0.10 \pm 0.01$	-0.01 ± 0.01

are consistent with zero within errors. Projections of the fits are shown in Figs. 1–3. The systematic errors from fitting are estimated from the deviations in \mathcal{A}_{CP} after varying each parameter of the signal PDFs by 1 standard deviation. The uncertainty in modeling the three-body background is studied by excluding the low ΔE region (< -0.12 GeV) and repeating the fit. Systematic uncertainties due to particle identification are estimated by checking the fit after varying the K/π efficiencies and fake rates by 1 standard deviation. At each step, the deviation in \mathcal{A}_{CP} is added in quadrature to provide the systematic errors, which are less than 0.01 for all modes. A possible bias from the fitting procedure is checked in MC and a bias due to the \mathcal{R} cut is investigated using the $B^+ \rightarrow \bar{D}^0 \pi^+$ samples. No significant bias is observed. The systematic uncertainties due to the detector bias are obtained using the fit results for the continuum background listed in Table II. The final systematic errors are

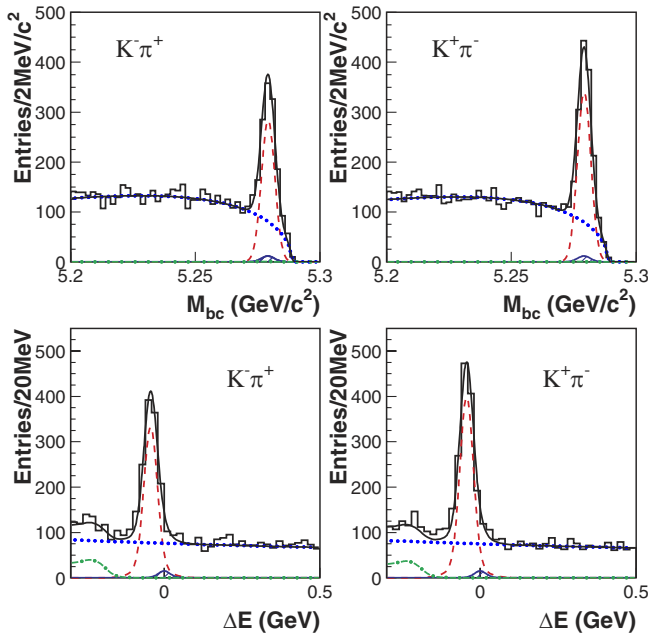


FIG. 1 (color online). M_{bc} (top) and ΔE (bottom) distributions for $\bar{B}^0 \rightarrow K^- \pi^+$ (left) and $B^0 \rightarrow K^+ \pi^-$ (right) candidates. The histograms represent the data, while the curves represent the various components from the fit: signal (dashed), continuum (dotted), three-body B decays (dash-dotted), background from misidentification (hatched), and sum of all components (solid).

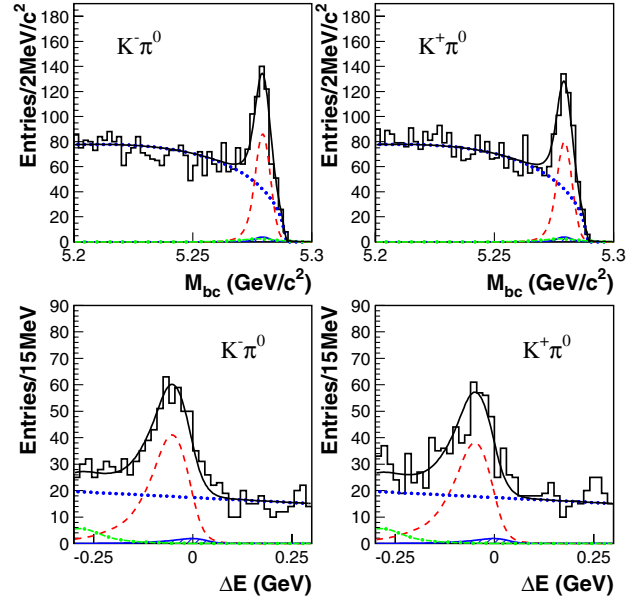


FIG. 2 (color online). M_{bc} (top) and ΔE (bottom) distributions for $B^- \rightarrow K^- \pi^0$ (left) and $B^+ \rightarrow K^+ \pi^0$ (right) candidates. The curves are described in the caption of Fig. 1.

then obtained by quadratically summing the errors due to the detector bias and the fitting systematics.

The partial rate asymmetry $\mathcal{A}_{CP}(K^+ \pi^-)$ is found to be $-0.101 \pm 0.025 \pm 0.005$, which is 3.9σ from zero. The significance calculation includes the effects of systematic uncertainties. Our result is consistent with the value reported by *BABAR*, $\mathcal{A}_{CP}(K^+ \pi^-) = -0.133 \pm 0.030 \pm 0.009$ [7]. The combined experimental result has a sig-

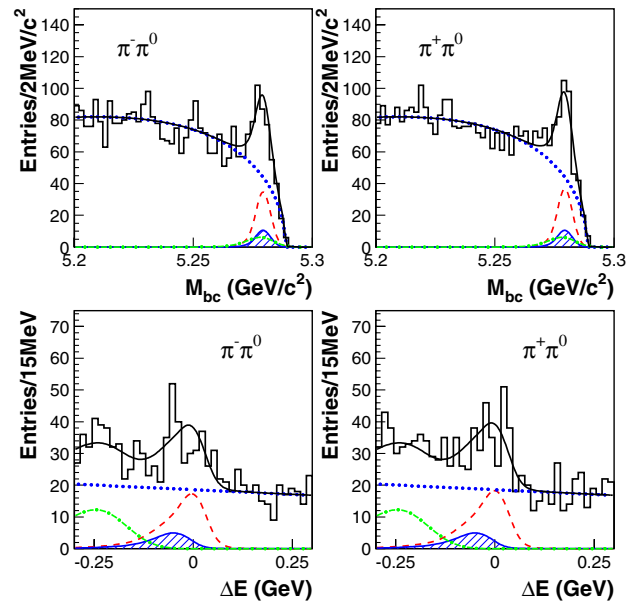


FIG. 3 (color online). M_{bc} (top) and ΔE (bottom) distributions for $B^- \rightarrow \pi^- \pi^0$ (left) and $B^+ \rightarrow \pi^+ \pi^0$ (right) candidates. The curves are described in the caption of Fig. 1.

nificance greater than 5σ , indicating that direct CP violation in the B meson system is established. Our measurement of $\mathcal{A}_{CP}(K^+\pi^0)$ is consistent with no asymmetry; the central value is 2.4σ away from $\mathcal{A}_{CP}(K^+\pi^-)$. If this result is confirmed with higher statistics, the difference may be due to the contribution of the electroweak penguin diagram or other mechanisms [16]. No evidence of direct CP violation is observed in the decay $B^+ \rightarrow \pi^+\pi^0$. We set 90% C.L. intervals $-0.05 < \mathcal{A}_{CP}(K^+\pi^0) < 0.13$ and $-0.18 < \mathcal{A}_{CP}(\pi^+\pi^0) < 0.14$.

We thank the KEKB group for the excellent operation of the accelerator, the KEK Cryogenics group for the efficient operation of the solenoid, and the KEK computer group and the NII for valuable computing and SuperSINET network support. We acknowledge support from MEXT and JSPS (Japan); ARC and DEST (Australia); NSFC (Contract No. 10175071, China); DST (India); the BK21 program of MOEHRD and the CHEP SRC program of KOSEF (Korea); KBN (Contract No. 2P03B 01324, Poland); MIST (Russia); MESS (Slovenia); NSC and MOE (Taiwan); and DOE (USA).

*On leave from Nova Gorica Polytechnic, Nova Gorica.

- [1] Belle Collaboration, K. Abe *et al.*, Phys. Rev. D **66**, 071102(R) (2002).
- [2] BABAR Collaboration, B. Aubert *et al.*, Phys. Rev. Lett. **89**, 201802 (2002).
- [3] M. Bander, D. Silverman, and A. Soni, Phys. Rev. Lett. **43**, 242 (1979).
- [4] Belle Collaboration, K. Abe *et al.*, Phys. Rev. Lett. **93**, 021601 (2004).
- [5] C.-K. Chua, W.-S. Hou, and K.-C. Yang, Mod. Phys. Lett. A **18**, 1763 (2003); S. Barshay, L. M. Sehgal, and J. van Leusen, Phys. Lett. B **591**, 97 (2004).
- [6] Belle Collaboration, Y. Chao *et al.*, hep-ex/0407025 [Phys. Rev. D. (to be published)].
- [7] BABAR Collaboration, B. Aubert *et al.*, hep-ex/0407057 [Phys. Rev. Lett. (to be published)].
- [8] Y.-Y. Keum and A. I. Sanda, Phys. Rev. D **67**, 054009 (2003); M. Beneke *et al.*, Nucl. Phys. B **606**, 245 (2001).
- [9] S. Kurokawa and E. Kikutani, Nucl. Instrum. Methods Phys. Res., Sect. A **499**, 1 (2003), and other papers included in this volume.
- [10] Belle Collaboration, A. Abashian *et al.*, Nucl. Instrum. Methods Phys. Res., Sect. A **479**, 117 (2002).
- [11] Belle SVD2 Group, Y. Ushiroda, Nucl. Instrum. Methods Phys. Res., Sect. A **511**, 6 (2003).
- [12] Belle Collaboration, Y. Chao *et al.*, Phys. Rev. D **69**, 111102(R) (2004).
- [13] The Fox-Wolfram moments were introduced in G. C. Fox and S. Wolfram, Phys. Rev. Lett. **41**, 1581 (1978). The modified moments used in this paper are described in Belle Collaboration, S. H. Lee *et al.*, Phys. Rev. Lett. **91**, 261801 (2003).
- [14] H. Kakuno *et al.*, hep-ex/0403022.
- [15] ARGUS Collaboration, H. Albrecht *et al.*, Phys. Lett. B **241**, 278 (1990).
- [16] A. J. Buras, R. Fleischer, S. Recksiegel, and F. Schwab, hep-ph/0402112; V. Barger, C.W. Chiang, P. Langacker, and H. S. Lee, Phys. Lett. B **598**, 218 (2004).